NCR-1 and NCR-2, the *C. elegans* homologs of the human Niemann-Pick type C1 disease protein, function upstream of DAF-9 in the dauer formation pathways

Jie Li, Gemma Brown, Michael Ailion*, Samuel Lee and James H. Thomas†

Department of Genome Sciences, University of Washington, Seattle, WA 98195, USA
*Present address: Institute of Neuroscience, University of Oregon, Eugene, OR 97403, USA
†Author for correspondence (e-mail: jht@u.washington.edu)

Summary

Mutations in the human NPC1 gene cause most cases of Niemann-Pick type C (NP-C) disease, a fatal autosomal recessive neurodegenerative disorder. NPC1 is implicated in intracellular trafficking of cholesterol and glycolipids, but its exact function remains unclear. The *C. elegans* genome contains two homologs of NPC1, *ncr-1* and *ncr-2*, and an *ncr-2; ncr-1* double deletion mutant forms dauer larvae constitutively (Daf-c). We have analyzed the phenotypes of *ncr* single and double mutants in detail, and determined the *ncr* gene expression patterns. We find that the *ncr* genes function in a hormonal branch of the dauer formation pathway upstream of *daf-9* and *daf-12*, which encode a cytochrome P450 enzyme and a nuclear hormone receptor, respectively. *ncr-1* is expressed broadly in tissues with high levels of cholesterol, whereas expression of *ncr-2* is restricted to a few cells. Both Ncr genes are expressed in the XXX cells, which are implicated in regulating dauer formation via the *daf-9* pathway. Only the *ncr-1* mutant is hypersensitive to cholesterol deprivation and to progesterone, an inhibitor of intracellular cholesterol trafficking. Our results support the hypothesis that *ncr-1* and *ncr-2* are involved in intracellular cholesterol processing in *C. elegans*, and that a sterol-signaling defect is responsible for the Daf-c phenotype of the *ncr-2; ncr-1* mutant.

Key words: Dauer, Niemann-Pick type C disease, Cholesterol, Hormone, *C. elegans*

Introduction

The diverse cellular functions of cholesterol require transport mechanisms that partition it to appropriate subcellular compartments. In mammalian cells, the endosome/lysosome system is crucial for redistributing cholesterol after endocytosis of low-density lipoproteins (Liscum and Munn, 1999). Human NPC1 is thought to be involved in this redistribution process. Defects in NPC1 are the cause of the fatal Niemann-Pick type C1 (NP-C1) disease, an autosomal recessive neurodegenerative disorder (Carstea et al., 1997; Loftus et al., 1997; Vanier and Millat, 2003). Loss of NPC1 function causes accumulation of unesterified cholesterol in the trans-Golgi network (TGN) and abnormal lysosome-like structures (Blanchette-Mackie et al., 1988; Pentchev et al., 1986). The NPC1 gene encodes a membrane glycoprotein with homology to the *Drosophila* morphogen receptor Patched (Ptc) and the bacterial RND family of transporters (Ioannou, 2000). One current model of NPC1 function is that it acts as a molecular pump for retrograde vesicular transport of lysosomal cargoes including cholesterol (Davies et al., 2000).

The *C. elegans* genome contains two homologs of the human NPC1 gene, *ncr-1* and *ncr-2* (NPC1 related genes), formerly known as *npc-1* and *npc-2*, respectively (Sym et al., 2000). Both *ncr* gene products have 31% identity with human NPC1 and contain all the structural domains of NPC1 (Sym et al.,

2000), including an N-terminal NPC1 domain and a sterol-sensing domain (SSD) (Chun and Simoni, 1992). *C. elegans* requires cholesterol in the growth medium (Chitwood, 1999), but little is known about the biological pathways mediating the uptake of cholesterol and subsequent processing and distributing steps (Kurzchalia and Ward, 2003). Nonetheless, the sequence conservation between human NPC1 and worm *ncr* genes suggests that an intracellular sterol trafficking pathway might be conserved.

A *C. elegans* model for NP-C1 disease was established by creating deletion mutations in both Ncr genes. Both deletions cause early frameshift mutations, and are thus likely to be null alleles. Although the single *ncr-1* and *ncr-2* mutants have subtle phenotypes, the *ncr-2; ncr-1* double mutant has a strong dauer formation constitutive (Daf-c) phenotype (Sym et al., 2000).

C. elegans dauers are alternative third-stage larvae that form in response to stressful environmental cues (Cassada and Russell, 1975; Riddle and Albert, 1997). Mutations in dauer formation (*daf*) genes result in either failure to form dauers in response to dauer inducing stimuli (dauer formation defective, or Daf-d), or constitutive formation of dauer larvae (dauer formation constitutive, or Daf-c). The *daf* genes function in complex parallel signaling pathways, including a cGMP pathway (Ailion and Thomas, 2000; Birnby et al., 2000; Coburn and Bargmann, 1996; Komatsu et al., 1996), a TGF-β

signaling pathway (Ren et al., 1996; Schackwitz et al., 1996) and an insulin pathway (Kimura et al., 1997; Li et al., 2003; Lin et al., 1997; Ogg et al., 1997). The outputs of these pathways are thought to be integrated by the nuclear hormone receptor DAF-12. Recently, elements of a hormonal pathway that probably acts on DAF-12 have been identified. They include a cytochrome P450 enzyme encoded by *daf-9* (Gerisch et al., 2001; Jia et al., 2002) and a PTP (protein tyrosine phosphatase)-like protein encoded by *sdf-9* (Ohkura et al., 2003). The DAF-9 protein is hypothesized to catalyze a step in the biosynthesis of a sterol ligand that inhibits the dauer promoting activity of the DAF-12 receptor. Loss-of-function mutants of *daf-9* share the pleiotropic developmental phenotypes of class 6 alleles of *daf-12*, which are thought to abolish ligand binding (Antebi et al., 1998; Antebi et al., 2000). SDF-9 is thought to augment or facilitate DAF-9 function (Ohkura et al., 2003). *daf-9* and *sdf-9* are co-expressed in a pair of head cells with possible neuroendocrine characteristics, called XXX cells (Ohkura et al., 2003). Killing the XXX cells induced dauer formation in wild-type animals and this cellular function was mapped to the same position in the dauer pathway as mutations in *sdf-9* (Gerisch et al., 2001; Ohkura et al., 2003).

We present evidence that *ncr-1* and *ncr-2* are involved in processing cholesterol, and that they function upstream of *daf-9* and *daf-12* in regulating dauer formation. We demonstrate that the expression pattern of *ncr-1* largely coincides with the pattern of cholesterol tissue distribution in *C. elegans* (Matyash et al., 2001; Merris et al., 2003), while the expression of *ncr-2* is more restricted. Both *ncr-1* and *ncr-2* are expressed in the XXX cells. The *ncr-1* mutant is sensitive to cholesterol deprivation (Sym et al., 2000) and to progesterone, an inhibitor of intracellular cholesterol trafficking. We propose that *ncr-1* is involved in sterol trafficking in general and that *ncr-1* and *ncr-2* function together in the XXX cells to affect the synthesis of the dauer-regulating sterol hormone.

Materials and methods

Culture conditions and strains
Strains were cultured using standard methods (Brenner, 1974). Normal NGM agar contained 5 μg/ml added cholesterol, low-sterol NGM plates omitted the cholesterol, and high-sterol NGM plates contained 20 μg/ml to 40 μg/ml added cholesterol. Cholesterol was added as 5 mg/ml or 10 mg/ml stock, dissolved in ethanol. Control plates in the same experiments always contained an equivalent volume of ethanol. *Escherichia coli* strain OP50 (TJ2) was used as a food source for worms (Ailion and Thomas, 2000). JT10654, the *ncr-2; ncr-1* strain we received from Dr Carl Johnson (Sym et al., 2000), contained a background mutation *osm-3(sa1206)*, which apparently masked many of the developmental phenotypes of *ncr-2; ncr-1* mutants. JT10800, the *ncr-2; ncr-1* strain used here, was rebuilt from the two single mutants and further outcrossed three times. The *ncr-1* and *ncr-2* strains were also outcrossed three times.

Assays
When continuously propagated, the *ncr-2; ncr-1* strain became progressively less healthy. This effect was apparent in poor recovery from the dauer and adult sterility. By contrast, worms that were freshly recovered from starved plates were much healthier and fecund. A similar phenomenon was reported for heterochronic mutants (Antebi et al., 1998; Liu and Ambros, 1991). In order to minimize variability between experiments, all assays involving the *ncr-2; ncr-1* strain used worms that were recovered from starved plates or their progeny. For

example, in media sterol assays, *ncr-2; ncr-1* mutants from starved NGM plates were allowed to recover on the assay plates, and noted as the starting generation (Gen 0). Dauer formation was scored for Gen 1 and Gen 2 progeny. Gen 1 progeny were also scored for dauer recovery, life span and brood size. Control strains in the same assays were treated in the same way.

For dauer formation assays, 6-10 adult hermaphrodites were allowed to lay eggs at room temperature (about 22°C) for 2-6 hours and then incubated at the assay temperature. Dauer and non-dauer animals were scored after 72-80 hours at 20°C, 54-60 hours at 25°C and 44-48 hours at 27°C. Brood size and life span assays were conducted at 20°C as described (Gems et al., 1998), for all strains except *ncr-2; ncr-1*. The zero time point was the time of the L4 transfer. The number of progeny was scored daily and then summed to get the total brood size. Similar procedures were followed for *ncr-2; ncr-1*, except that dauers from staged egg-lays were used in the assays instead of L4 larvae. In this case, the zero point was the time of dauer transfer. Samples that died from internal hatching of embryos or from exploded vulva were included in the graphs. Statistical analyses including Student's *t*-test and the Kruskal-Wallis non-parametric ANOVA test were performed using InStat2.01.

Non-complementation screen for new *ncr-1* alleles
ncr-2(nr2023) males were mutagenized by EMS (Sulston and Hodgkin, 1988), and allowed to recover overnight. These males were crossed to *ncr-2(nr2023); ncr-1(nr2022) lon-2(e678)* or to *ncr-2(nr2023); ncr-1(nr2022) lon-2(e678) daf-12(m20)*. Non-Lon dauers were picked in the F1 and new *ncr-1* alleles were made homozygous by selecting F2 animals that segregated no Lon progeny.

Sequencing and cloning cDNAs
The gene structure of *ncr-1* was deduced by sequencing the yk39e8 cDNA clone. The gene structure of *ncr-2* was deduced by sequencing RT-PCR products generated by gene specific primers. The 5′ end of both genes were determined by sequencing PCR products amplified with SL1 leader sequence and gene specific primers. For *ncr-2*, the 3′ end was determined by sequencing 3′ RACE products amplified by gene specific primers and adapter primers (Invitrogen).

Germline transformation
Germline transformation was carried out as described (Mello et al., 1991), at a concentration of 5-50 ng/ml test DNA with 5-50 ng/ml co-injection marker [*myo-2p*::*gfp*, or pBLH98(*lin-15+*)] and 50-80 ng/ml carrier DNA [pBluescript KS(+)].

Single gene rescue and reporter constructs
A 13 kb *Kpn*I fragment of cosmid F02E8 containing the *ncr-1A* coding region with 3288 bp of upstream promoter sequence was sufficient to rescue the Daf-c phenotype of the *ncr-2; ncr-1* mutant (see Table S1 in the supplementary material). A PCR fragment containing the *ncr-2* coding region, with 1084 bp of upstream promoter sequence, was sufficient to rescue the Daf-c phenotype of the *ncr-2; ncr-1* mutant (see Table S1 in the supplementary material). A PCR fragment containing the *daf-9a* coding region with 1947 bp of promoter sequence was used for DAF-9 overexpression studies.

The vectors pPD95.75 and TJ1665 (the dsRed2 derivative of pPD95.69) were used to study the gene expression patterns. pTJ1665 was made by substituting dsRed2 cDNA for the GFP-coding sequence of pPD95.69, removing the nuclear localization signal of pPD95.69 in the process. A 3540 bp fragment of *ncr-1A* promoter was amplified and cloned into the *Sph*I and *Xma*I sites of pPD95.75 to generate plasmid pTJ1663 [*ncr-1Ap(s)::gfp*]. A longer 8709 bp fragment of *ncr-1A* promoter was used similarly to generate plasmid pTJ1726 [*ncr-1Ap(l)::gfp*]. For the rarer *ncr-1B* transcript, a 6571 bp fragment of *ncr-1B* promoter was amplified and cloned into pPD95.75 to generate plasmid pTJ1727(*ncr-1Bp::gfp*). For *ncr-2*, a 4568 bp promoter fragment was amplified and cloned into pPD95.75 to make

plasmid pTJ1664 (*ncr-2p::gfp*). For plasmid pTJ1728 (*ncr-2p::dsRed2*), the *Pst*I-*Xma*I promoter fragment from pTJ1664 was blunted at the *Pst*I site and cloned into the *Hin*cII and *Xma*I sites of pTJ1665.

Behavioral assays

Osmotic avoidance assays were performed as described (Culotti and Russell, 1978) by testing whether animals crossed a ring of 8 M glycerol during 10 minute assays. Chemotaxis toward the volatile attractive odorants and NaCl was assayed as described (Bargmann et al., 1993; Bargmann and Horvitz, 1991).

Imaging

Fluorescent dye-filling assays were performed as described (Fujiwara et al., 1999; Hedgecock et al., 1985) using DiI-C12 (Molecular Probes, Eugene, OR). Dye-filled animals were observed at 1000× magnification by conventional fluorescence microscopy (Zeiss Axioskop). To capture the 3D morphology of ASER neuron, freshly formed dauer larvae of the *ncr-2; ncr-1* genotype and wild-type L3 larvae were set up for observation as described (Swoboda et al., 2000). 3D data stacks were acquired in the FITC channel by moving the focal plane in 0.5 μm increments through the entire worm. Background and out-of-focus signal were removed using a conservative, reiterative (15×) deconvolution algorithm (Agard et al., 1989; Scalettar et al., 1996). 3D data stacks were combined using maximum intensity projections of all data points along the *z*-axis.

Results

Pleiotropic phenotype of the *ncr-2; ncr-1* mutant

The *ncr-2; ncr-1* double mutant animals display developmental phenotypes similar to *daf-9* and *daf-12* class 6 mutants (Antebi et al., 1998; Gerisch et al., 2001; Jia et al., 2002). Like them, the dauer-like larvae formed by *ncr-2; ncr-1* had a pharynx that was partially constricted and continued to pump, the germline continued proliferating, and they were paler and more mobile than normal dauers (Fig. 1A-C). In addition, *ncr-2; ncr-1* was also able to

form normal dauers in response to starvation or dauer pheromone (data not shown). Under reproductive growth conditions, *ncr-2; ncr-1* animals recovered spontaneously from the dauer-like stage and exhibited pleiotropic developmental phenotypes as adults.

The brood size and life span of *ncr-2; ncr-1* mutants were reduced (Fig. 2B,C) and most *ncr-2; ncr-1* adults showed vulval abnormalities (80%, *n*=49). In less severe cases (47%), the animals had an abnormally protruding vulva (Fig. 1G); in more severe cases (33%), the uterus everted through the vulval opening. Probably owing to the vulval defects, *ncr-2; ncr-1* animals had an egg-laying defective (Egl-d) phenotype: 29% (*n*=49) eventually died from internal hatching of larvae (Fig. 1G). However, even after excluding worms that died from an erupted vulva or internal hatching of larvae, the *ncr-2; ncr-1* mutant still produced fewer progeny (91.2±76.6, *n*=16) than did the wild type (315.5±51.4, *n*=40), indicating some additional fertility defect. The cuticle alae of *ncr-2; ncr-1* adults sometimes missed segments (28.9%, *n*=38), a phenotype that suggests defective seam cell development (Fig. 1E). *ncr-2; ncr-1* mutants also exhibited a low frequency gonadal migration phenotype (3.1%, *n*=162).

To summarize, *ncr-2; ncr-1* share most of the pleiotropic phenotypes of *daf-9* and class 6 *daf-12* mutants, including formation of characteristic partial dauers, abnormal vulval morphology and defects in seam cell development and distal tip cell migration. In each case, the phenotype of *ncr-2; ncr-1* is less severe than most *daf-9* and *daf-12* mutants, indicating that *ncr-2; ncr-1* causes a similar but less severe underlying defect.

Fig. 1. Pleiotropic phenotypes of *ncr-2; ncr-1* mutants. (A-C) Characteristic morphology of *ncr-2; ncr-1* dauer-like larvae. (A) *ncr-2(nr2023); ncr-1(nr2022)* dauer-like larva. (B) *daf-9(m540)* dauer-like larva. (C) *daf-7(e1372)* dauer larva. Left and right panels show the pharynx and the alae, respectively. In the left panels, the black and white arrowheads indicate the isthmus and the terminal bulb of the pharynx. Compared with the fully constricted pharynx of a *daf-7* dauer, which is similar to normal dauers, those of the *ncr-2; ncr-1* and *daf-9* mutants are only partially constricted. In the right panels, the black arrowheads indicate the dauer lateral alae consisting of morphologically distinct longitudinal ridges. (D-G) Pleiotropic developmental phenotypes of *ncr-2; ncr-1* adults. (D) In a young wild-type adult, normal alae consist of three or four parallel longitudinal ridges. (E) Broken alae in an *ncr-2; ncr-1* adult. White arrowheads indicate the remaining faint alae up to the point where they are broken. (F) Normal vulval morphology of a wild-type adult. The vulva is a slightly protruding structure, forming the opening through which fertilized eggs are expelled from the uterus. (G) Abnormal vulval morphology of a *ncr-2; ncr-1* mutant. The white arrow indicates the vulval protrusion and black arrowheads indicate late stage embryos about to hatch inside the parent. Scale bars: 20 μm.
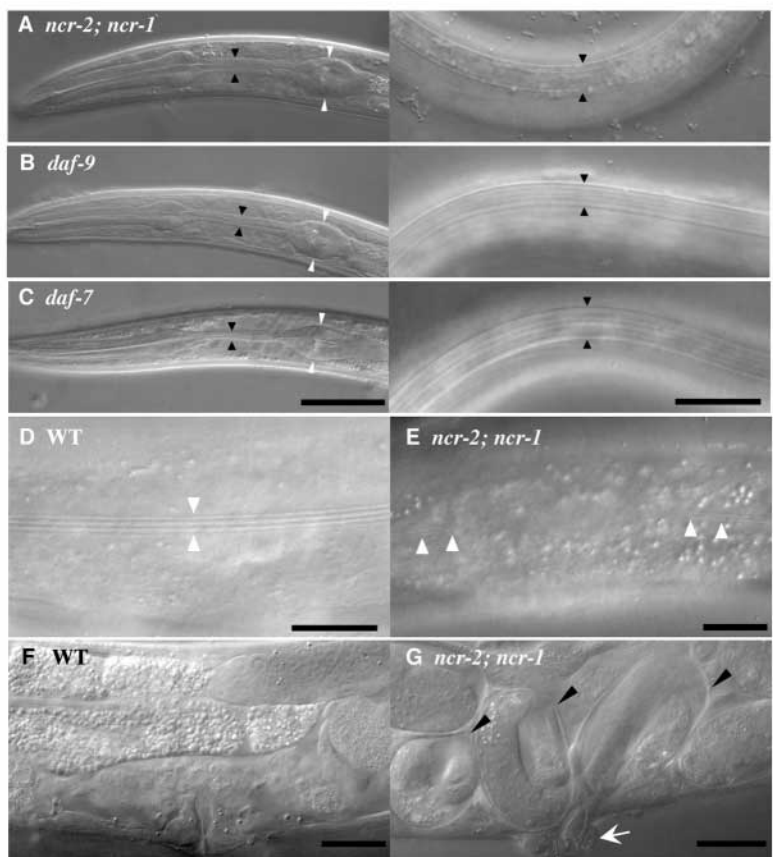
High media cholesterol rescues *ncr-2; ncr-1* mutants

Because the NPC proteins are involved in trafficking sterols in mammals, we tested whether raising the media cholesterol concentration could rescue the *ncr-2; ncr-1* mutant. The Daf-c phenotype of the *ncr-2; ncr-1* mutant was significantly suppressed by raising the level of cholesterol in the media (Fig. 2A). High cholesterol also promoted recovery from dauer arrest and ameliorated the post-dauer phenotypes, as demonstrated by improved brood size and lengthened average life span (Fig. 2B,C). Increasing media cholesterol had no obvious effect on the dauer formation phenotype of other Daf-c mutants, including *daf-9*, *daf-2* and *daf-7* (Fig. 2A), though the recovery of *daf-9* dauers was mildly promoted (Jia et al., 2002) (data not shown). These results suggest that cholesterol availability is limiting in *ncr-2; ncr-1*, but not in the other Daf-c mutants, consistent with an NCR function in delivering sterol substrates to the DAF-9 enzyme.

In order to identify possible substrates and products of the DAF-9 enzyme, we tested the ability of other sterols and steroids to suppress the Daf-c phenotype of the *ncr-2; ncr-1* mutant. Because it is abundant in fungi and plants and can substitute for cholesterol to sustain the growth and reproduction of the worm (Chitwood, 1999), ergosterol is a likely sterol source for *C. elegans* in the wild. Pregnenolone is the product of the first side-chain cleavage of cholesterol, the rate-limiting step in mammalian steroid biosynthesis (Simpson, 1979). We also tested the insect molting hormone ecdysone and a human steroid hormone progesterone. Only ergosterol moderately rescued the Daf-c phenotype of *ncr-2; ncr-1*, whereas ecdysone and pregnenolone had no effect (data not shown). Intriguingly, adding progesterone to normal NGM plates retarded the larval development of the *ncr-2; ncr-1* mutant and inhibited its recovery from the dauer stage (data not shown). We decided to further examine the effect of progesterone.

ncr-1 mutants are sensitive to progesterone in the growth media

Progesterone can inhibit intracellular cholesterol trafficking in mammalian cells (Butler et al., 1992; Liscum and Munn, 1999). In fibroblast cell cultures, it causes accumulation of unesterified cholesterol in abnormal lysosome-like compartments, the same cellular phenotype that characterizes NP-C1 disease. Multiple steps of cholesterol intracellular trafficking appear to be affected by progesterone, but the exact mechanism and the targets of its action remain unknown.

To determine whether progesterone also disturbs cholesterol trafficking in *C. elegans*, we examined its effect on wild-type worms. Wild-type worms grown on NGM plates that contained 20 μg/ml progesterone in addition to the normal 5 μg/ml cholesterol developed into fertile adults. However, when progesterone was added to low-sterol NGM plates, pleiotropic phenotypes similar to those caused by cholesterol deprivation (Gerisch et al., 2001; Merris et al., 2003) were observed (Fig. 3). Many animals were defective in gonadal tip cell migration (54%, *n*=37), with both gonadal arms extending ventrally, failing to make the programmed turns (Fig. 3B). Frequently, sperm were observed in the pseudocoelomic space (39%, *n*=23), probably owing to a disrupted basement membrane (Fig. 3D). Occasional dauer larvae were also observed.
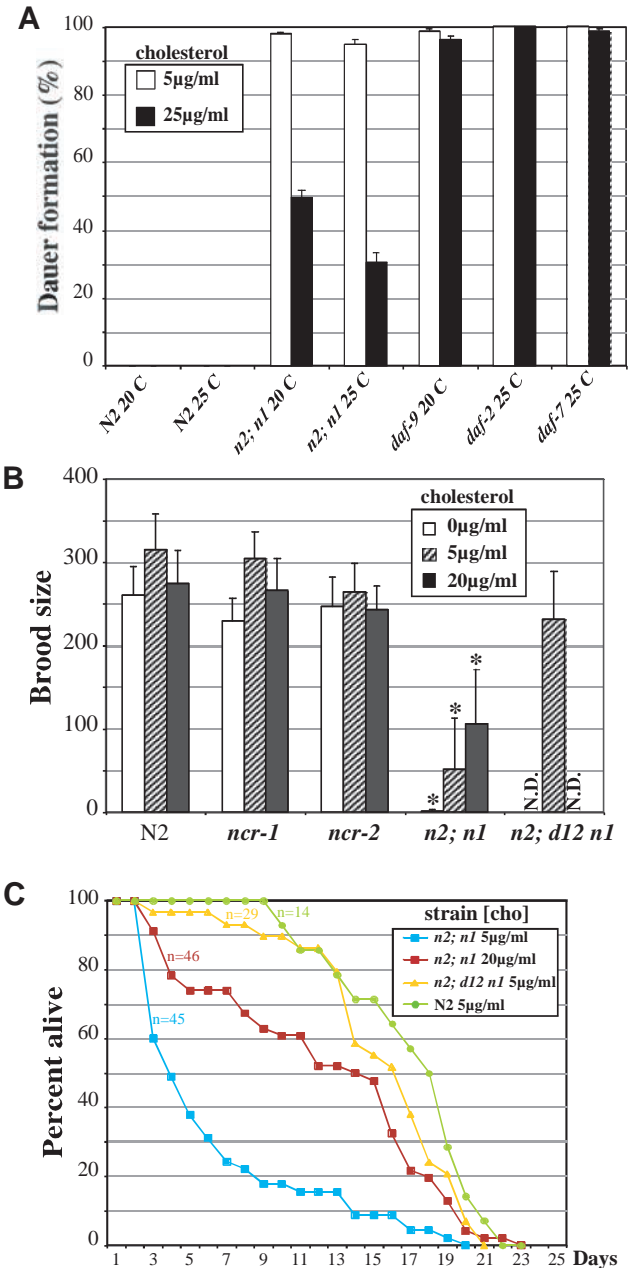
The *ncr-1* single and *ncr-2; ncr-1* double mutants were

Fig. 2. Cholesterol is at limiting concentration in *ncr-2; ncr-1* mutants. Higher cholesterol levels suppress the Daf-c phenotype of *ncr-2; ncr-1*, but not the other Daf-c mutants, including *daf-2(e1370ts)*, *daf-7(e1372ts)* and *daf-9(m540)*. The dauer formation of Gen 2 worms is presented here (see Materials and methods). The error bars indicate the s.d. values of binomial populations. (B) The brood size of *ncr-2; ncr-1* mutant is enhanced by higher cholesterol levels. *$P<0.0001$, Kruskal-Wallis nonparametric ANOVA test. (C) The average life span (±s.d.) of recovered *ncr-2; ncr-1* dauers on plates containing 5 μg/ml and 20 μg/ml cholesterol is 7.7±5.1 days and 12.9±6.2 days respectively, $P<0.0001$, Student's *t*-test. The experiments in B,C were conducted at 20°C. *n2; n1* is *ncr-2(nr2023); ncr-1(nr2022)* and *n2; d12 n1* is *ncr-2(nr2023); daf-12(m20) ncr-1(nr2022)*.

hypersensitive to progesterone treatment (Fig. 4). On low-sterol NGM plates containing 20 μg/ml progesterone, 77% (*n*=120) of *ncr-1* and 85% (*n*=94) of *ncr-2; ncr-1* mutants died

Fig. 3. Progesterone treatment of wild-type worms mimics phenotypes caused by cholesterol deprivation. (A,C) Normaski micrographs of wild-type worms grown on normal plates. (B,D) Normaski micrographs of representative wild-type worms cultured on low-sterol NGM plates containing 20 µg/ml progesterone. The phenotypes of Gen 1 adults are presented (see Materials and methods). (A) Normal gonadal cell migration. (B) Abnormal gonadal cell migration in animals cultured on progesterone plates. The distal tip cell migrated on the ventral side all the way up to the pharynx, failing to make either of the programmed turns. The black arrow indicates the direction of dtc migration. (C) Under normal conditions, the sperm (white arrowheads) are enclosed within spermatheca (sp). (D) Loose sperm in N2 animals cultured on progesterone plates. White arrowheads indicate sperm found within pseudocoelomic space, probably owing to rupture of the basement membrane surrounding the somatic gonad. Scale bars: 20 µm.
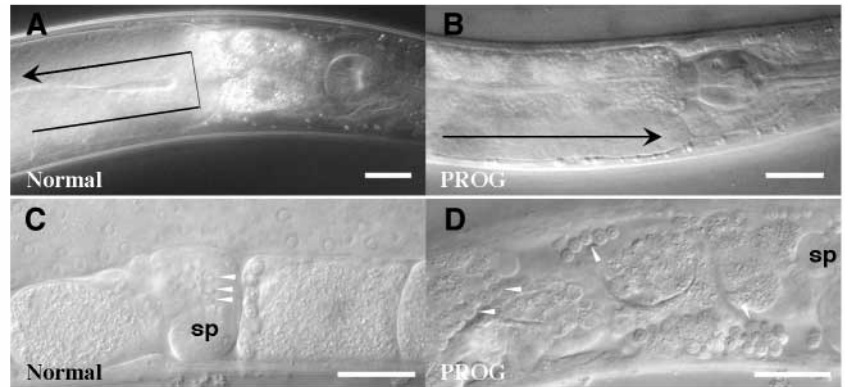
prematurely as early larvae, with the remainder arrested in L1/L2 larval stages. By contrast, *ncr-2* single mutants were no more sensitive to progesterone treatment than were the wild type. These results are consistent with the previous observations that *ncr-1* and *ncr-2; ncr-1* mutants but not *ncr-2* mutants were hypersensitive to cholesterol deprivation (Sym et al., 2000). The toxic effect of progesterone was prevented by a normal concentration (5 µg/ml) of cholesterol in the media, suggesting that progesterone specifically affects cholesterol trafficking in *C. elegans*.

Gene structures of *ncr-1* and *ncr-2*

We deduced the coding sequence of the *ncr-1* gene through a combination of sequencing cDNA clones and overlapping RT-PCR products. Two SL1 spliced transcripts *ncr-1A* and *ncr-1B* were identified; *ncr-1B* contains an additional 96 bp first exon located 8.7 kb upstream of the first exon of *ncr-1A* (Fig. 5A). The first exon of *ncr-1B* contains termination codons and does not contain any additional translational start codons in frame with the downstream protein coding sequence, and therefore is likely to be non-coding. The *ncr-1B* transcript was under-represented in the RT-PCR products, suggesting that it is the minor transcript. Both transcripts would give rise to a protein of 1383 amino acids, corresponding to the predicted protein product.

Two additional mutations in *ncr-1* were isolated from a non-complementation screen. *sa1420* is a C to T transition which results in a premature stop codon in exon 13. *sa1421* is a missense mutation in which one of the conserved cysteines, C997, of the cysteine-rich loop is replaced by a tyrosine. A cluster of human disease mutations are located in this region of the protein. Similar to the deletion allele *nr2022*, both *sa1420* and *sa1421* confer a strong Daf-c phenotype in combination with *ncr-2(nr2023)* (Table 1), indicating that they are strong loss-of-function or null mutations.

A single SL1 spliced transcript for *ncr-2* was identified from sequencing overlapping RT-PCR products (Fig. 5C). The results confirm the previously predicted gene structure.

Expression patterns of *ncr-1* and *ncr-2* genes

We used promoter GFP fusions to study the expression patterns of the *ncr-1* and *ncr-2* genes. Three reporter constructs, *ncr-1Ap(s)::gfp*, *ncr-1Ap(l)::gfp* and *ncr-1Bp::gfp* were made for *ncr-1* because of its complex gene structure (Fig. 5B). The results indicate that *ncr-1* expression is widespread (Fig. 5B) and largely coincides with the reported distribution pattern of cholesterol in *C. elegans*, which includes the following tissues: intestine, pharynx, excretory gland cell, nerve ring, spermatheca and germ cells, including both oocytes and sperm (Matyash et al., 2001; Merris et al., 2003). In the following sections, we summarize the observed *ncr-1* expression pattern within specific tissues.

Intestine

Both *ncr-1Ap(s)::gfp* and *ncr-1Ap(l)::gfp* were strongly expressed throughout the intestine (Fig. 6A), with posterior intestinal expression consistently stronger than anterior expression.
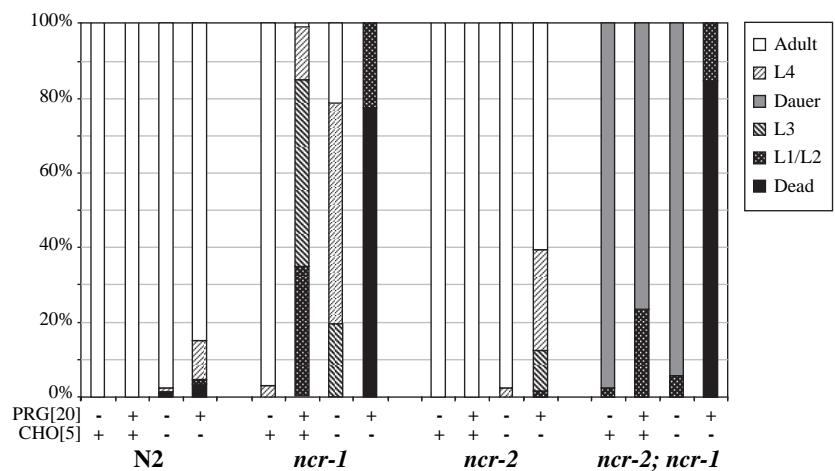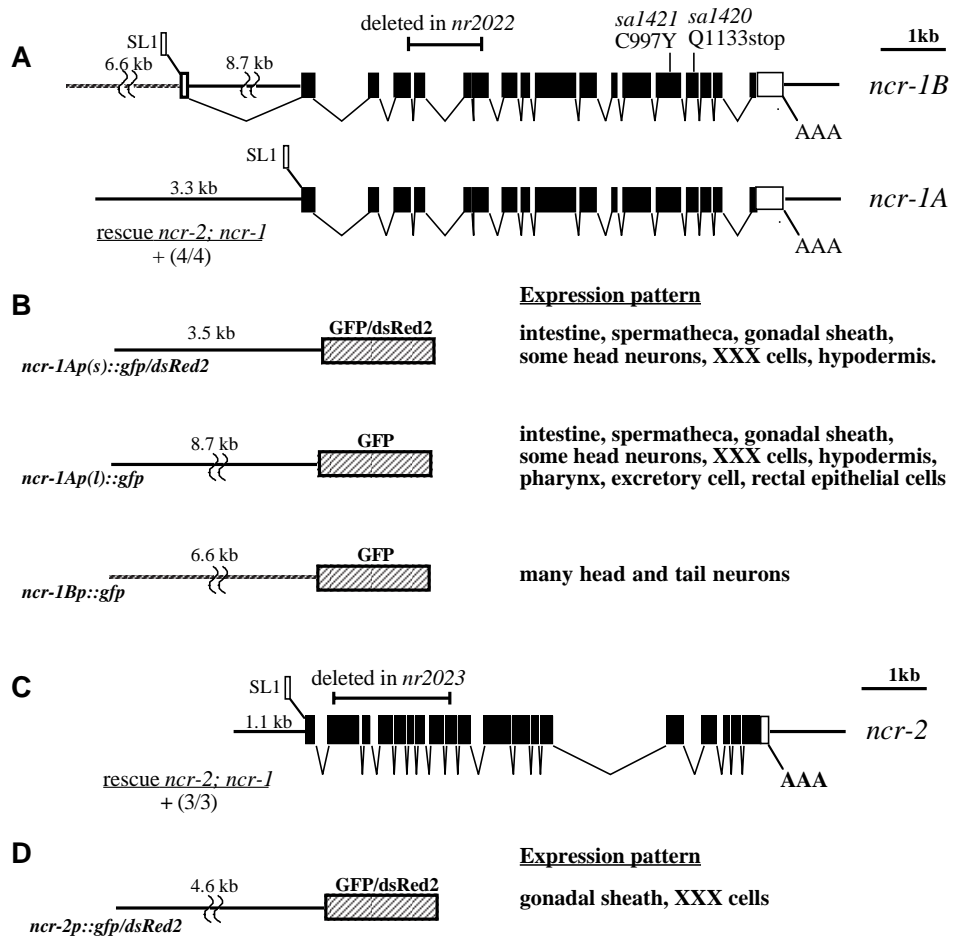

Fig. 4. *ncr-1* and *ncr-2; ncr-1* mutants are hypersensitive to progesterone. Synchronized populations of N2, *ncr-1*, *ncr-2*, or *ncr-2; ncr-1* strains (Gen 1, see Materials and methods) were cultured on NGM plates with (+) or without (–) 5 µg/ml cholesterol and 20 µg/ml progesterone. The development of wild-type and mutant worms were scored after 72 hours at 20°C. The results from duplicate experiments were pooled together and expressed as a percent value (*n*>50).

Musculature

ncr-1Ap(l)::gfp was strongly expressed in pharyngeal muscles (Fig. 6A,B), but not in body wall muscles.

Nervous system

ncr-1Ap(s)::gfp and *ncr-1Ap(l)::gfp* were expressed in the same set of head and tail neurons and a pair of neuron-like cells identified as the XXX cells (Fig. 6B,H) (Ohkura et al., 2003). According to their location and cellular morphology, we identified the head neurons as the pharyngeal neuron I6, the inner labial sensory neurons IL2s and the amphid neurons ASE and ASG. The expression level in the amphid neurons was weaker than in the other head neurons. The tail neurons were identified as PHC, in which expression was first detected during the L2 stage, consistent with the time of birth of the neurons at the end of L1. In contrast to the widespread expression of *ncr-1Ap::gfp*, *ncr-1Bp::gfp* is expressed exclusively in 10-12 pairs of head and tail neurons (Fig. 6K). The tail neurons were identified as PHA, PHB and DVC. One pair of head neurons was identified as AWC. The other head neurons were very tentatively identified as RIC, RIM, FLP, ADA, ADE, RID and maybe AIY. We also occasionally observed expression in a pair of head cells anterior to the nerve ring. The position and morphology of these cells are similar to the XXX cells.

With the exception of PHC neurons, expression in the tissues above was first observed during late embryogenesis and did not change during development.

Somatic gonad

Both *ncr-1Ap(s)::gfp* and *ncr-1Ap(l)::gfp* were strongly expressed in the spermatheca and weakly in the gonadal sheath cells (Fig. 6D). The expression in the somatic gonad could be observed only in adults.

Epidermis

ncr-1Ap(l)::gfp was strongly expressed in the excretory cell (Fig. 6A-C) and rectal epithelial cells (Fig. 6C) from the early

L1 larval stage and through all life stages. Seam cell expression was first observed in the late L1 stage (Fig. 6E), while expression in the lateral hypodermis increased during the L3 stage and peaked during the L4 stage (Fig. 6F). Seam cell and hypodermal expression gradually decreased in the adult stage and was hardly visible among older adults (Fig. 6G). *ncr-1Ap(s)::gfp* was not expressed in the hypodermis under normal growth conditions, though lateral hypodermal but not seam cell expression was dramatically upregulated in starved animals of all developmental stages (Fig. 6I,J). Similar upregulation of hypodermal expression in response to starvation has been reported for *daf-9* (Gerisch and Antebi, 2004). No increase in hypodermal expression was seen in starved *ncr-1Ap(l)::gfp* animals.

In contrast to the widespread expression of *ncr-1*, the expression of *ncr-2p::gfp* was restricted to the XXX cells and the somatic gonad. It was strongly expressed in the proximal gonadal sheath cells and weakly in the spermatheca (Fig. 6L). The XXX expression of *ncr-2p::gfp* was seen throughout development (Fig. 6M), while the gonadal expression was observed only in adults.

Position of *ncr* genes in the dauer formation pathway

To determine the position of *ncr* genes in the dauer pathway, we analyzed the dauer formation phenotypes of *daf-d; ncr-2; ncr-1* triple mutants (Table 2). Mutations in *osm-6*, *daf-5* and *daf-16* suppress the Daf-c phenotype of mutants in the cGMP,

Table 1. Additional alleles of *ncr-1* isolated from a non-complementation screen

	Dauer-like larva formation*		
Strain	15°C	20°C	25°C
Wild type (N2)	0% (146)	0% (30)	0% (69)
ncr-2(nr2023); ncr-1(nr2022)	100% (146)	100% (96)	100% (191)
ncr-2(nr2023); ncr-1(sa1420)	99% (163)	100% (120)	100% (77)
ncr-2(nr2023); ncr-1(sa1421)	100% (214)	100% (72)	99%(182)

*The numbers in parentheses show the total numbers of animals scored.

TGF-β and insulin pathways, respectively (Thomas et al., 1993; Vowels and Thomas, 1992). The Daf-c phenotype of *ncr-2; ncr-1* was not suppressed by *osm-6* and *daf-5* mutations, placing the *ncr* genes parallel to or downstream of these genes. A severe loss-of-function allele of *daf-16*, *m27*, did not suppress the *ncr-2; ncr-1* Daf-c phenotype, but the null allele *mgDf50* did suppress partially, suggesting that *daf-16* might be a minor downstream target of the *ncr* genes. The loss-of-function allele *daf-12(m20)*, completely suppressed the Daf-c and the pleiotropic post-dauer phenotypes of *ncr-2; ncr-1* mutant (Fig. 2B,C), placing the function of the *ncr* genes upstream of *daf-12* and also suggesting that the pleiotropic post-dauer phenotypes of *ncr-2; ncr-1* result from unregulated DAF-12 activity. This pathway position for the *ncr* genes is the same as *daf-9* (Gerisch et al., 2001; Jia et al., 2002), suggesting that the *ncr* genes function in the hormonal branch of the dauer formation pathway.

Overexpression of DAF-9 activity rescues the *ncr-2; ncr-1* Daf-c phenotype

We tested the effect of overexpressing DAF-9 activity in the *ncr-2; ncr-1* mutant (Table 3). Expressing a wild-type *daf-9* fully suppressed the Daf-c phenotype of *ncr-2; ncr-1*, and
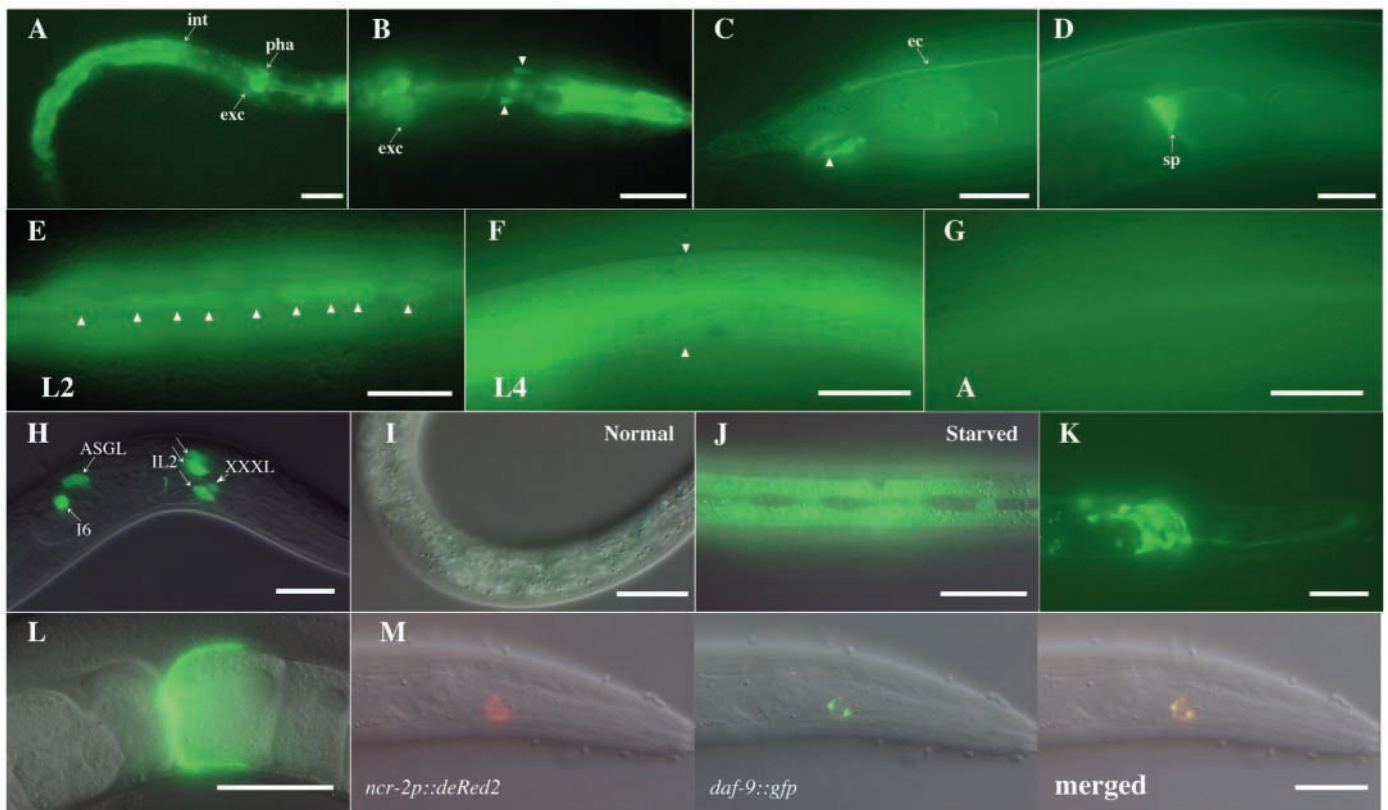

Fig. 6. Expression patterns of *ncr-1* and *ncr-2*. (A-G) Expression pattern of the *ncr-1Ap(l)::gfp* construct. (A) Pharynx (pha), excretory cell (exc), and intestine (int) strongly express GFP, in an L1/L2 larva. (B) Enlarged view of the head region in A. Two out of the six IL2 neurons are in focus, indicated by arrowheads. The other head neurons are out of focus or obscured by strong fluorescence from the pharynx. (C) Expression in the excretory canal (ec, arrow) and rectal epithelial cells (arrowhead). (D) GFP is strongly expressed in the spermatheca (sp) of an adult worm, and also weakly expressed in the gonadal sheath and uterus wall. (E-G) Dynamic hypodermal expression of *ncr-1Ap(l)::gfp* during development. (E) GFP expression is first observed in the lateral hypodermal seam cells during late L1/early L2 stages. Individual seam cells are indicated by white arrowheads. (F) By the L4 stage, the entire hypodermis, consisting of seam cells and the lateral hypodermis, expresses GFP. White arrowheads indicate the edge of the lateral hypodermis. (G) After the L4/adult molt, the hypodermal expression diminishes. (H-J) Expression pattern of *ncr-1Ap(s)::gfp* fusion. (H) Expression in identified head neurons, including three out of the six IL2 neurons (the other three are out of focus), ASGL, pharyngeal neuron I6 and XXXL cell. (I,J) Starvation induces strong GFP expression in lateral hypodermis, but not in seam cells. Shown here are L2 stage larvae from normal growth conditions (I) and from a plate that has been starved for 12-24 hours (J). (K) The *ncr-1Bp::gfp* fusion is expressed in about 10 pairs of head neurons, in an L1 stage larva. (L,M) Expression pattern of *ncr-2p::gfp*. (L) In an adult animal, *ncr-2p::gfp* is strongly expressed in proximal gonadal sheath cells and weakly expressed in spermatheca. (M) *ncr-2p::dsRed2* expression (left) colocalizes with *daf-9::gfp* (middle) in the XXX cells. *ncr-2p::dsRed2* is expressed diffusely throughout the cells, compared with the perinuclear pattern of *daf-9::gfp* expression. In the merged view (right), *daf-9::gfp* is pseudocolored yellow to reveal the red color better. Scale bars: 20 μm.

ectopic expression of DAF-9 activity in the hypodermis also significantly suppressed the phenotype. By contrast, overexpressing NCR-1 or NCR-2 activities failed to suppress the dauer formation phenotype of *daf-9(m540)* (Table S1). These results suggest that NCR proteins function upstream of DAF-9 in the dauer formation pathway.

Genetic interaction with *sdf-9* mutants

The PTP (protein tyrosine phosphatase)-like protein encoded by *sdf-9* is another likely component of the hormonal branch of the dauer formation pathway. At elevated culture temperature, loss-of-function alleles of *sdf-9* exhibit an impenetrant Daf-c phenotype: they form characteristic dauer-like larvae that spontaneously recover (Ohkura et al., 2003). Like *ncr-2; ncr-1* mutants, *sdf-9* mutants are sensitive to cholesterol levels in the culture media, which led us to examine *sdf-9* interactions with *ncr-1* and *ncr-2* (Table 4). At 25°C, all three tested alleles of *sdf-9* were strongly Daf-c with the *ncr-1* mutation, but not the *ncr-2* mutation.

Neuronal phenotypes of *ncr* mutants

Most individuals with NP-C present neurological symptoms of late-infantile or juvenile onset, accompanied by substantial neuronal loss in specific brain regions (Vanier and Millat, 2003). To determine whether the NCR proteins are also required for neuronal function in *C. elegans*, we evaluated neuronal morphology using cell specific GFP markers or by direct dye filling, and measured neuronal function by quantitative behavioral assays.

A morphological defect was observed in the ASER neuron (*gcy-5::gfp*) (Yu et al., 1997): during the transient dauer stage, ASER often (69.2%, *n*=13) had an ectopic posterior process terminating in one or more swellings (Fig. 7A). The defect appeared to be transient because it was absent during the early larval stages, peaked during dauer stage, then regressed as dauers recovered (Fig. 7B). This structural change was not observed in dauers formed by wild-type worms on starved plates, nor in dauers formed by the *daf-7(e1372)* mutant, and therefore was not caused by dauer arrest itself. Moreover, this morphological defect in ASER was not observed in *ncr-1* or *ncr-2* single mutants growing reproductively or in dauers induced by starvation, suggesting that it is specifically associated with the transient dauer stage of the *ncr-2; ncr-1* double mutant.

The structure of many amphid and phasmid neurons can be visualized using lipophilic dyes (Fujiwara et al., 1999; Hedgecock et al., 1985). We examined the morphology of the dye-filled neurons in newly formed *ncr-2; ncr-1* dauers. The phasmid neurons were normal in all animals examined (*n*=47), but a significant proportion of the mutant animals (68%, *n*=47) contained one or more amphid neurons with a morphological abnormality similar to the ASER neuron. Of the labeled neurons, ASJ seemed to be most severely affected (Table S2).

ASE and the dye-filled head neurons are all amphid neurons. We examined other types of neurons, including interneuron AIY (*ttx-3::gfp*) (Hobert et al., 1997), sensory neurons BAG (*gcy-33::gfp*) (Yu et al., 1997), IL2 (*ncr-1Ap(s)::gfp*) and GABAergic motoneurons (*unc-25::gfp*) (Jin et al., 1999). A small proportion (18%, *n*=33) of *ncr-2; ncr-1* mutant animals exhibited an AIY defect similar to that observed in ASER during the transient dauer stage. No defect was observed in the

Table 2. Dauer-like larva formation in *daf-d; ncr-2; ncr-1* mutants

Strain	Dauer-like larva formation*		
	15°C	20°C	25°C
Wild type (N2)	0% (699)	0% (317)	0% (702)
ncr-2(nr2023); ncr-1(nr2022)	91% (447)	91% (842)	99% (455)
ncr-2; osm-6(p811); ncr-1	98% (581)	98% (413)	100% (219)
daf-5(e1385); ncr-2; ncr-1	100% (673)	100% (791)	99%(474)
daf-5(e1386); ncr-2; ncr-1	99% (928)	99% (320)	100% (383)
daf-16(m27); ncr-2; ncr-1	99% (117)	99% (141)	99% (172)
daf-16(mgDf50); ncr-2; ncr-1	77% (753)	58% (390)	55% (736)
daf-12(m20); ncr-2; ncr-1	0% (456)	0% (806)	0% (779)

*The numbers in parentheses show the total numbers of animals scored.

Table 3. Suppression of the Daf-c phenotype of *ncr-2; ncr-1* by *daf-9(+)* transgene

Transgene array	Dauer-like larva formation at 20°C*	
	+Ex†	–Ex†
daf-9(+)		
Line 1	0% (182)	65% (204)
Line 2	0% (68)	56% (91)
Line 3	0% (84)	76% (62)
dpy-7p::daf-9 cDNA::gfp		
Line 1	14% (7)	83% (98)
Line 2	3% (106)	84% (103)
Line 3	1% (174)	78% (60)

*The numbers in parentheses show the total numbers of animals scored.
†+Ex and –Ex refers to individuals that contain or do not contain the trangene arrays, as indicated by the presence or absence of the co-injection marker *myo-2p::gfp*.

Table 4. Genetic interactions of *ncr-1* and *ncr-2* with *sdf-9*

Strain	Dauer-like larva formation*	
	20°C	25°C
N2	0% (314)	0% (296)
ncr-1(nr2022)	0% (212)	0% (353)
ncr-2(nr2023)	0% (221)	0% (280)
ncr-2; ncr-1	84% (622)	99% (554)
sdf-9 (ut163)	0% (217)	11% (200)
sdf-9 (ut169)	1% (181)	16% (225)
sdf-9 (ut187)	1% (149)	44% (182)
ut163; ncr-1	2% (769)	98% (483)
ut169; ncr-1	87% (393)	97% (174)
ut187; ncr-1	63% (817)	99% (443)
ncr-2; ut163	0% (549)	19% (493)
ncr-2; ut169	0% (626)	15% (486)
ncr-2; ut187	0% (498)	7% (562)

*The numbers in parentheses show the total numbers of animals scored.

other neuron classes during or after the transient dauer stage. We conclude that NCR function is required to maintain the morphological integrity of some but not all neurons during the transient dauer stage and that amphid neurons as a class may be more severely affected than other neurons.

Many amphid neurons function in regulating dauer formation and in chemotaxis response to soluble and volatile environmental stimuli, including a major role for ASE neurons in chemotaxis towards NaCl (Bargmann and Horvitz, 1991). To assess the function of amphid neurons, we measured the avoidance response of *ncr-2; ncr-1* adults to high osmotic strength and their chemotaxis response to NaCl, diacetyl,
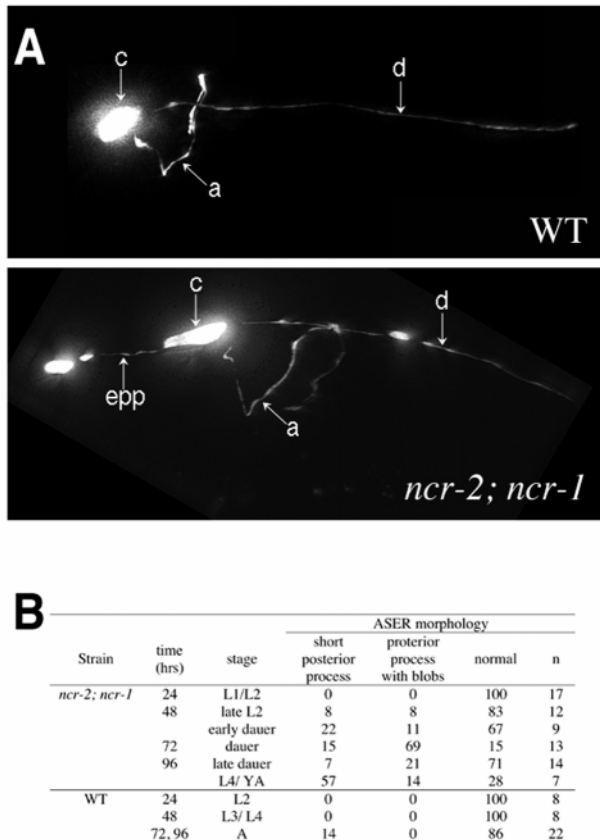
Fig. 7. Morphological abnormality of the ASER neuron in the *ncr-2; ncr-1* mutant. (A) GFP labeled wild-type and mutant ASER neurons. The wild-type ASER neuron (top panel) consists of a cell body (c), a dendritic process (d) to the amphid sensory organ in the nose, and an axon process (a) to the nerve ring. The bottom panel shows the morphology of an ASER neuron of the *ncr-2; ncr-1* mutant at the dauer stage. The mutant neuron sends out an ectopic posterior process (epp), often terminating in one or more swellings. (B) The morphological defect of the ASER neuron in *ncr-2; ncr-1* mutant is transient and associated with the dauer stage. The percent value of each morphological class is reported.

isoamyl alcohol, and 2, 4, 5-trimethylthiazole (Bargmann et al., 1993; Bargmann and Horvitz, 1991). *ncr-2; ncr-1* mutants exhibited robust responses towards all the above stimuli, indicating normal neuronal function. However, the *ncr-2; ncr-1* adult animals used in these assays were recovered from starved plates. Ideally, the behaviors should be assessed in animals that have undergone the transient dauer stage, but this was impractical because of complications from the pleiotropic developmental phenotypes. We also measured the same behavioral responses in the *ncr* single and *ncr-2; ncr-1; daf-12* triple mutant adult animals grown under normal conditions, and found that these mutants also had wild-type responses.

Discussion

Genetic position of *ncr* genes in the dauer formation pathway

Our genetic analysis suggests that *ncr-1* and *ncr-2* function upstream of *daf-9* and *daf-12* in a hormonal branch of the dauer

formation pathway. First, the *ncr-2; ncr-1* double mutant has pleiotropic phenotypes similar to *daf-9* and Daf-c alleles of *daf-12*. Second, epistasis analysis places the *ncr-1* and *ncr-2* genes upstream of *daf-12* and parallel or downstream to the other dauer formation pathways, the same position as *daf-9*. Finally, overexpressing DAF-9 suppressed the Daf-c phenotype of the *ncr-2; ncr-1* mutant, but overexpressing NCR-1 or NCR-2 failed to suppress *daf-9(m540)* phenotypes, indicating that the *ncr* genes function upstream of *daf-9*.

The molecular identities of the *ncr* and *daf-9* genes suggest a model in which NCR proteins are required for redistributing internalized cholesterol to intracellular compartments, including the endoplasmic reticulum (ER). The DAF-9 cytochrome P450 enzyme, which appears to be ER localized (Gerisch et al., 2001; Jia et al., 2002), may depend on sterol substrates delivered by the NCR pathway for the biosynthesis of a DAF-12 ligand (Gerisch and Antebi, 2004; Mak and Ruvkun, 2004). In *ncr-2; ncr-1* mutants, defective sterol trafficking results in reduced availability of DAF-9 substrates, thus recapitulating the pleiotropic phenotypes of *daf-9* and *daf-12* class 6 (ligand binding domain) mutants. This model predicts a suboptimal concentration of available cholesterol in the *ncr-2; ncr-1* mutant, but a normal or higher available cholesterol concentration in the *daf-9* mutant. Rescue of *ncr-2; ncr-1* by increased exogenous cholesterol is consistent with this model.

Expression pattern of *ncr* genes

Two cDNA isoforms of *ncr-1* were identified in this study. They differ only in their 5′-UTR region caused by an alternative non-coding first-exon located 8.7 kb upstream of the predicted coding region. A sequence homologous to this non-coding exon is located 9.4 kb upstream of the predicted *C. briggsae ncr-1* gene in a similar arrangement, suggesting functional significance. The expression pattern of the *ncr-1* gene reveals two interesting features. First, the *ncr-1* gene expression pattern largely coincides with the tissue distribution of cholesterol in *C. elegans* (Matyash et al., 2001; Merris et al., 2003), consistent with a function for NCR-1 in cholesterol trafficking. Second, the hypodermal expression of the *ncr-1* gene is dynamically regulated by developmental and environmental signals. A similar dynamic regulation of *daf-9* expression has been reported (Gerisch and Antebi, 2004; Gerisch et al., 2001).

The expression of *ncr-1* and *ncr-2* colocalizes with *daf-9* and *sdf-9* in a pair of neuroendocrine cells called XXX cells (Ohkura et al., 2003). In previous studies, ablating the XXX cells caused the formation of characteristic partial dauers, suggesting that these cells are an important source of the dauer-inhibiting hormone (Ohkura et al., 2003). It was proposed that SDF-9 functions by increasing DAF-9 activity or helping to execute DAF-9 function (Ohkura et al., 2003). We hypothesize that *sdf-9* participates in a signal transduction cascade that modulates the output of the *daf-9* pathway in concert with intracellular sterol levels. We found that *sdf-9* is strongly Daf-c in combination with *ncr-1*, but not with *ncr-2* mutations. This result can be explained by two alternative models. In the first, NCR-1 and NCR-2 function redundantly in the XXX cells in cholesterol trafficking, but NCR-1 plays a more important role than NCR-2. Alternatively, NCR-1 is involved in cholesterol trafficking, whereas NCR-2 functions at a different step in the

dauer signaling pathway, perhaps parallel or downstream to SDF-9 function. The broader expression of NCR-1, as well as its sensitivity towards cholesterol deprivation and progesterone, suggests a major role in cholesterol trafficking. However, further studies, such as determining the subcellular localization of the NCR proteins, are necessary to help resolve the two models.

The DAF-12 ligand

The current study supports the hypothesis that a hormone ligand for DAF-12 is derived from sterol. It has previously been shown that lack of DAF-9 function could not be bypassed by the addition of exogenous pregnenolone (Jia et al., 2002), suggesting that it is not the product of the DAF-9 enzyme. We find that pregnenolone fails to alleviate the phenotypes of the *ncr-2; ncr-1* mutant, suggesting that pregnenolone or its derivatives are also unlikely to be the substrates of the DAF-9 enzyme. Pregnenolone is the precursor of vertebrate steroid hormones and the product of the first side-chain cleavage of cholesterol. Consistent with our results, the *C. elegans* genome contains no recognizable ortholog of mammalian cytochrome P450scc, which catalyzes the complex multi-step reaction of pregnenolone synthesis (Simpson, 1979).

The insect molting hormone ecdysone is structurally different from vertebrate steroid hormones. It contains the sterol multi-ring system and an intact side chain, which is modified by oxidation (mostly hydroxylations) and methylation at multiple positions (Gilbert et al., 2002). As a result, ecdysone is amphipathic, a property that helps its movement across cell boundaries and diffusion through tissues. Although the pathway for ecdysone biosynthesis has not been fully characterized, cytochrome P450 enzymes are likely to catalyze many of the hydroxylation steps (Gilbert et al., 2002). Interestingly, it was recently reported that the levels of hydroxycholesterols are diminished in cell lines lacking NPC1 function, and among different mutant NPC1 lines, hydroxycholesterol levels correlate better with the severity of cellular phenotypes than do ER cholesterol levels (Frolov et al., 2003). It is possible that the hormonal ligand of DAF-12 is structurally more similar to the insect hormone ecdysone, with an intact side chain and modified by hydroxylations, than to the vertebrate steroid hormones.

C. elegans as a model system to study NPC1 function

Mammalian pathways for intracellular cholesterol trafficking are probably conserved in *C. elegans*. In addition to *ncr-1* and *ncr-2*, the *C. elegans* genome contains an ortholog of the human NPC2/HE1 gene, the locus responsible for the remaining 5% of cases of NP-C disease (Friedland et al., 2003; Ko et al., 2003; Naureckiene et al., 2000). The *C. elegans* genome also contains homologs of LDL-receptor-like proteins (Grant and Hirsh, 1999; Ishihara et al., 2002; Yochem et al., 1999), caveolin (Scheel et al., 1999), START domain proteins, a large family of cytochrome P450 enzymes (Menzel et al., 2001) and more than 250 nuclear hormone receptors (Gissendanner et al., 2004).

Progesterone inhibits intracellular cholesterol trafficking in mammalian cell lines. We show that progesterone probably also inhibits cholesterol trafficking in *C. elegans*. First, progesterone treatment phenocopied the effects of cholesterol

deprivation in wild-type animals; second, *ncr-1* mutants were hypersensitive to progesterone treatment; and third, the effects of progesterone could be suppressed by cholesterol in the media. However, NCR proteins are unlikely to be the direct targets of progesterone, as progesterone treatment of either single mutant failed to phenocopy the *ncr-2; ncr-1* double mutant.

In mammalian cells, intracellular trafficking of cholesterol and sphingolipid are closely linked (Puri et al., 1999; Zhang et al., 2001). Complex glycosphingolipids accumulate in NPC cells in addition to cholesterol (Neufeld et al., 1999; Zhang et al., 2001). It has been hypothesized that the neurological symptoms of NPC disease are caused by sphingolipid accumulation, because they accumulate more extensively than cholesterol in the central nervous system, and because the neuropathological changes in NPC disease resemble those in primary sphingolipid storage disorders (Liu et al., 2000; Zervas et al., 2001b). Although little is known about the metabolism and homeostasis of sphingolipids in *C. elegans*, we find neuronal abnormalities in *ncr-2; ncr-1* mutants similar to the ectopic dendritogenesis observed in the mammalian NPC disease models, which is thought to be caused by accumulation of the ganglioside GM2 (Walkley, 1998; Zervas et al., 2001a).

In conclusion, *C. elegans* represents a useful model organism for studying conserved pathways of intracellular cholesterol trafficking. Classical genetic approaches and genome-wide screening methods can be employed to identify additional components that interact with the *ncr* genes and to yield potential therapeutic targets for the treatment of NP-C disease.

Supplementary material

Supplementary material for this article is available at http://dev.biologists.org/cgi/content/full/131/22/5741/DC1

References

Agard, D. A., Hiraoka, Y., Shaw, P. and Sedat, J. W. (1989). Fluorescence microscopy in three dimensions. *Methods Cell Biol.* **30**, 353-377.

Ailion, M. and Thomas, J. H. (2000). Dauer formation induced by high temperatures in *Caenorhabditis elegans*. *Genetics* **156**, 1047-1067.

Antebi, A., Culotti, J. G. and Hedgecock, E. M. (1998). *daf-12* regulates developmental age and the dauer alternative in *Caenorhabditis elegans*. *Development* **125**, 1191-1205.

Antebi, A., Yeh, W. H., Tait, D., Hedgecock, E. M. and Riddle, D. L. (2000). *daf-12* encodes a nuclear receptor that regulates the dauer diapause and developmental age in *C. elegans*. *Genes Dev.* **14**, 1512-1527.

Bargmann, C. I. and Horvitz, H. R. (1991). Chemosensory neurons with overlapping functions direct chemotaxis to multiple chemicals in *C. elegans*. *Neuron* **7**, 729-742.

Bargmann, C. I., Hartwieg, E. and Horvitz, H. R. (1993). Odorant-selective genes and neurons mediate olfaction in *C. elegans*. *Cell* **74**, 515-527.

Birnby, D. A., Link, E. M., Vowels, J. J., Tian, H., Colacurcio, P. L. and Thomas, J. H. (2000). A transmembrane guanylyl cyclase (DAF-11) and Hsp90 (DAF-21) regulate a common set of chemosensory behaviors in *Caenorhabditis elegans*. *Genetics* **155**, 85-104.

Blanchette-Mackie, E. J., Dwyer, N. K., Amende, L. M., Kruth, H. S., Butler, J. D., Sokol, J., Comly, M. E., Vanier, M. T., August, J. T., Brady, R. O. et al. (1988). Type-C Niemann-Pick disease: low density lipoprotein uptake is associated with premature cholesterol accumulation in the Golgi complex and excessive cholesterol storage in lysosomes. *Proc. Natl. Acad. Sci. USA* **85**, 8022-8026.

Brenner, S. (1974). The genetics of *Caenorhabditis elegans*. *Genetics* **77**, 71-94.

Butler, J. D., Blanchette-Mackie, J., Goldin, E., O'Neill, R. R., Carstea, G., Roff, C. F., Patterson, M. C., Patel, S., Comly, M. E., Cooney, A. et al. (1992). Progesterone blocks cholesterol translocation from lysosomes. *J. Biol. Chem.* **267**, 23797-23805.

Carstea, E. D., Morris, J. A., Coleman, K. G., Loftus, S. K., Zhang, D., Cummings, C., Gu, J., Rosenfeld, M. A., Pavan, W. J., Krizman, D. B. et al. (1997). Niemann-Pick C1 disease gene: homology to mediators of cholesterol homeostasis. *Science* **277**, 228-231.

Cassada, R. C. and Russell, R. L. (1975). The dauer larva, a post-embryonic developmental variant of the nematode *Caenorhabditis elegans*. *Dev. Biol.* **46**, 326-342.

Chitwood, D. J. (1999). Biochemistry and function of nematode steroids. *Crit. Rev. Biochem. Mol. Biol.* **34**, 273-284.

Chun, K. T. and Simoni, R. D. (1992). The role of the membrane domain in the regulated degradation of 3-hydroxy-3-methylglutaryl coenzyme A reductase. *J. Biol. Chem.* **267**, 4236-4246.

Coburn, C. M. and Bargmann, C. I. (1996). A putative cyclic nucleotide-gated channel is required for sensory development and function in *C. elegans*. *Neuron* **17**, 695-706.

Culotti, J. G. and Russell, R. L. (1978). Osmotic avoidance defective mutants of the nematode *Caenorhabditis elegans*. *Genetics* **90**, 243-256.

Davies, J. P., Chen, F. W. and Ioannou, Y. A. (2000). Transmembrane molecular pump activity of Niemann-Pick C1 protein. *Science* **290**, 2295-2298.

Friedland, N., Liou, H. L., Lobel, P. and Stock, A. M. (2003). Structure of a cholesterol-binding protein deficient in Niemann-Pick type C2 disease. *Proc. Natl. Acad. Sci. USA* **100**, 2512-2517.

Frolov, A., Zielinski, S. E., Crowley, J. R., Dudley-Rucker, N., Schaffer, J. E. and Ory, D. S. (2003). NPC1 and NPC2 regulate cellular cholesterol homeostasis through generation of low density lipoprotein cholesterol-derived oxysterols. *J. Biol. Chem.* **278**, 25517-25525.

Fujiwara, M., Ishihara, T. and Katsura, I. (1999). A novel WD40 protein, CHE-2, acts cell-autonomously in the formation of *C. elegans* sensory cilia. *Development* **126**, 4839-4848.

Gems, D., Sutton, A. J., Sundermeyer, M. L., Albert, P. S., King, K. V., Edgley, M. L., Larsen, P. L. and Riddle, D. L. (1998). Two pleiotropic classes of *daf-2* mutation affect larval arrest, adult behavior, reproduction and longevity in *Caenorhabditis elegans*. *Genetics* **150**, 129-155.

Gerisch, B. and Antebi, A. (2004). Hormonal signals produced by DAF-9/cytochrome P450 regulate *C. elegans* dauer diapause in response to environmental cues. *Development* **131**, 1765-1776.

Gerisch, B., Weitzel, C., Kober-Eisermann, C., Rottiers, V. and Antebi, A. (2001). A hormonal signaling pathway influencing *C. elegans* metabolism, reproductive development, and life span. *Dev. Cell* **1**, 841-851.

Gilbert, L. I., Rybczynski, R. and Warren, J. T. (2002). Control and biochemical nature of the ecdysteroidogenic pathway. *Annu. Rev. Entomol.* **47**, 883-916.

Gissendanner, C. R., Crossgrove, K., Kraus, K. A., Maina, C. V. and Sluder, A. E. (2004). Expression and function of conserved nuclear receptor genes in *Caenorhabditis elegans*. *Dev. Biol.* **266**, 399-416.

Grant, B. and Hirsh, D. (1999). Receptor-mediated endocytosis in the *Caenorhabditis elegans* oocyte. *Mol. Biol. Cell* **10**, 4311-4326.

Hedgecock, E. M., Culotti, J. G., Thomson, J. N. and Perkins, L. A. (1985). Axonal guidance mutants of *Caenorhabditis elegans* identified by filling sensory neurons with fluorescein dyes. *Dev. Biol.* **111**, 158-170.

Hobert, O., Mori, I., Yamashita, Y., Honda, H., Ohshima, Y., Liu, Y. and Ruvkun, G. (1997). Regulation of interneuron function in the *C. elegans* thermoregulatory pathway by the *ttx-3* LIM homeobox gene. *Neuron* **19**, 345-357.

Ioannou, Y. A. (2000). The structure and function of the Niemann-Pick C1 protein. *Mol. Genet. Metab.* **71**, 175-181.

Ishihara, T., Iino, Y., Mohri, A., Mori, I., Gengyo-Ando, K., Mitani, S. and Katsura, I. (2002). HEN-1, a secretory protein with an LDL receptor motif, regulates sensory integration and learning in *Caenorhabditis elegans*. *Cell* **109**, 639-649.

Jia, K., Albert, P. S. and Riddle, D. L. (2002). DAF-9, a cytochrome P450 regulating *C. elegans* larval development and adult longevity. *Development* **129**, 221-231.

Jin, Y., Jorgensen, E., Hartwieg, E. and Horvitz, H. R. (1999). The *Caenorhabditis elegans* gene *unc-25* encodes glutamic acid decarboxylase and is required for synaptic transmission but not synaptic development. *J. Neurosci.* **19**, 539-548.

Kimura, K. D., Tissenbaum, H. A., Liu, Y. and Ruvkun, G. (1997). *daf-2*, an insulin receptor-like gene that regulates longevity and diapause in *Caenorhabditis elegans*. *Science* **277**, 942-946.

Ko, D. C., Binkley, J., Sidow, A. and Scott, M. P. (2003). The integrity of a cholesterol-binding pocket in Niemann-Pick C2 protein is necessary to control lysosome cholesterol levels. *Proc. Natl. Acad. Sci. USA* **100**, 2518-2525.

Komatsu, H., Mori, I., Rhee, J. S., Akaike, N. and Ohshima, Y. (1996). Mutations in a cyclic nucleotide-gated channel lead to abnormal thermosensation and chemosensation in *C. elegans*. *Neuron* **17**, 707-718.

Kurzchalia, T. V. and Ward, S. (2003). Why do worms need cholesterol? *Nat. Cell Biol.* **5**, 684-688.

Li, W., Kennedy, S. G. and Ruvkun, G. (2003). *daf-28* encodes a *C. elegans* insulin superfamily member that is regulated by environmental cues and acts in the DAF-2 signaling pathway. *Genes Dev.* **17**, 844-858.

Lin, K., Dorman, J. B., Rodan, A. and Kenyon, C. (1997). *daf-16*: an HNF-3/forkhead family member that can function to double the life-span of *Caenorhabditis elegans*. *Science* **278**, 1319-1322.

Liscum, L. and Munn, N. J. (1999). Intracellular cholesterol transport. *Biochim. Biophys. Acta* **1438**, 19-37.

Liu, Y., Wu, Y. P., Wada, R., Neufeld, E. B., Mullin, K. A., Howard, A. C., Pentchev, P. G., Vanier, M. T., Suzuki, K. and Proia, R. L. (2000). Alleviation of neuronal ganglioside storage does not improve the clinical course of the Niemann-Pick C disease mouse. *Hum. Mol. Genet.* **9**, 1087-1092.

Lui, Z. and Ambros, V. (1991). Alternative temporal control systems for hypodermal cell differentiation in *Caenorhabditis elegans*. *Nature* **350**, 162-165.

Loftus, S. K., Morris, J. A., Carstea, E. D., Gu, J. Z., Cummings, C., Brown, A., Ellison, J., Ohno, K., Rosenfeld, M. A., Tagle, D. A. et al. (1997). Murine model of Niemann-Pick C disease: mutation in a cholesterol homeostasis gene. *Science* **277**, 232-235.

Mak, H. Y. and Ruvkun, G. (2004). Intercellular signaling of reproductive development by the *C. elegans* DAF-9 cytochrome P450. *Development* **131**, 1777-1786.

Matyash, V., Geier, C., Henske, A., Mukherjee, S., Hirsh, D., Thiele, C., Grant, B., Maxfield, F. R. and Kurzchalia, T. V. (2001). Distribution and transport of cholesterol in *Caenorhabditis elegans*. *Mol. Biol. Cell* **12**, 1725-1736.

Mello, C. C., Kramer, J. M., Stinchcomb, D. and Ambros, V. (1991). Efficient gene transfer in C. elegans: extrachromosomal maintenance and integration of transforming sequences. *EMBO J.* **10**, 3959-3970.

Menzel, R., Bogaert, T. and Achazi, R. (2001). A systematic gene expression screen of *Caenorhabditis elegans* cytochrome P450 genes reveals CYP35 as strongly xenobiotic inducible. *Arch. Biochem. Biophys.* **395**, 158-168.

Merris, M., Wadsworth, W. G., Khamrai, U., Bittman, R., Chitwood, D. J. and Lenard, J. (2003). Sterol effects and sites of sterol accumulation in *Caenorhabditis elegans*: developmental requirement for 4alpha-methyl sterols. *J. Lipid Res.* **44**, 172-181.

Naureckiene, S., Sleat, D. E., Lackland, H., Fensom, A., Vanier, M. T., Wattiaux, R., Jadot, M. and Lobel, P. (2000). Identification of HE1 as the second gene of Niemann-Pick C disease. *Science* **290**, 2298-2301.

Neufeld, E. B., Wastney, M., Patel, S., Suresh, S., Cooney, A. M., Dwyer, N. K., Roff, C. F., Ohno, K., Morris, J. A., Carstea, E. D. et al. (1999). The Niemann-Pick C1 protein resides in a vesicular compartment linked to retrograde transport of multiple lysosomal cargo. *J. Biol. Chem.* **274**, 9627-9635.

Ogg, S., Paradis, S., Gottlieb, S., Patterson, G. I., Lee, L., Tissenbaum, H. A. and Ruvkun, G. (1997). The Fork head transcription factor DAF-16 transduces insulin-like metabolic and longevity signals in *C. elegans*. *Nature* **389**, 994-999.

Ohkura, K., Suzuki, N., Ishihara, T. and Katsura, I. (2003). SDF-9, a protein tyrosine phosphatase-like molecule, regulates the L3/dauer

developmental decision through hormonal signaling in *C. elegans*. *Development* **130**, 3237-3248.

Pentchev, P. G., Kruth, H. S., Comly, M. E., Butler, J. D., Vanier, M. T., Wenger, D. A. and Patel, S. (1986). Type C Niemann-Pick disease. A parallel loss of regulatory responses in both the uptake and esterification of low density lipoprotein-derived cholesterol in cultured fibroblasts. *J. Biol. Chem.* **261**, 16775-16780.

Puri, V., Watanabe, R., Dominguez, M., Sun, X., Wheatley, C. L., Marks, D. L. and Pagano, R. E. (1999). Cholesterol modulates membrane traffic along the endocytic pathway in sphingolipid-storage diseases. *Nat. Cell Biol.* **1**, 386-388.

Ren, P., Lim, C. S., Johnsen, R., Albert, P. S., Pilgrim, D. and Riddle, D. L. (1996). Control of *C. elegans* larval development by neuronal expression of a TGF-beta homolog. *Science* **274**, 1389-1391.

Riddle, D. L. and Albert, P. S. (1997). Regulation of dauer larva development. In *C. elegans II* (ed. D. L. Riddle, T. Blumenthal, B. J. Meyer and J. R. Priess), pp. 739-768. Cold Spring Harbor, NY: Cold Spring Harbor Laboratory Press.

Scalettar, B. A., Swedlow, J. R., Sedat, J. W. and Agard, D. A. (1996). Dispersion, aberration and deconvolution in multi-wavelength fluorescence images. *J. Microsc.* **182**, 50-60.

Schackwitz, W. S., Inoue, T. and Thomas, J. H. (1996). Chemosensory neurons function in parallel to mediate a pheromone response in *C. elegans*. *Neuron* **17**, 719-728.

Scheel, J., Srinivasan, J., Honnert, U., Henske, A. and Kurzchalia, T. V. (1999). Involvement of caveolin-1 in meiotic cell-cycle progression in *Caenorhabditis elegans*. *Nat. Cell Biol.* **1**, 127-129.

Simpson, E. R. (1979). Cholesterol side-chain cleavage, cytochrome P450, and the control of steroidogenesis. *Mol. Cell. Endocrinol.* **13**, 213-227.

Sulston, J. and Hodgkin, J. (1988). Methods. In *The Nematode* Caenorhabditis elegans (ed. W. B. Wood), pp. 595. Cold Spring Harbor, NY: Cold Spring Harbor Laboratory Press.

Swoboda, P., Adler, H. T. and Thomas, J. H. (2000). The RFX-type transcription factor DAF-19 regulates sensory neuron cilium formation in *C. elegans*. *Mol. Cell* **5**, 411-421.

Sym, M., Basson, M. and Johnson, C. (2000). A model for Niemann-Pick type C disease in the nematode *Caenorhabditis elegans*. *Curr. Biol.* **10**, 527-530.

Thomas, J. H., Birnby, D. A. and Vowels, J. J. (1993). Evidence for parallel processing of sensory information controlling dauer formation in *Caenorhabditis elegans*. *Genetics* **134**, 1105-1117.

Vanier, M. T. and Millat, G. (2003). Niemann-Pick disease type C. *Clin. Genet.* **64**, 269-281.

Vowels, J. J. and Thomas, J. H. (1992). Genetic analysis of chemosensory control of dauer formation in *Caenorhabditis elegans*. *Genetics* **130**, 105-123.

Walkley, S. U. (1998). Cellular pathology of lysosomal storage disorders. *Brain Pathol.* **8**, 175-193.

Yochem, J., Tuck, S., Greenwald, I. and Han, M. (1999). A gp330/megalin-related protein is required in the major epidermis of *Caenorhabditis elegans* for completion of molting. *Development* **126**, 597-606.

Yu, S., Avery, L., Baude, E. and Garbers, D. L. (1997). Guanylyl cyclase expression in specific sensory neurons: a new family of chemosensory receptors. *Proc. Natl. Acad. Sci. USA* **94**, 3384-3387.

Zervas, M., Dobrenis, K. and Walkley, S. U. (2001a). Neurons in Niemann-Pick disease type C accumulate gangliosides as well as unesterified cholesterol and undergo dendritic and axonal alterations. *J. Neuropathol. Exp. Neurol.* **60**, 49-64.

Zervas, M., Somers, K. L., Thrall, M. A. and Walkley, S. U. (2001b). Critical role for glycosphingolipids in Niemann-Pick disease type C. *Curr. Biol.* **11**, 1283-1287.

Zhang, M., Dwyer, N. K., Neufeld, E. B., Love, D. C., Cooney, A., Comly, M., Patel, S., Watari, H., Strauss, J. F., III, Pentchev, P. G. et al. (2001). Sterol-modulated glycolipid sorting occurs in niemann-pick C1 late endosomes. *J. Biol. Chem.* **276**, 3417-3425.